Exceptional Electronic Modulation of Porphyrins through *meso*-Arylethynyl Groups. Electronic Spectroscopy, Electronic Structure, and Electrochemistry of [5,15-Bis[(aryl)ethynyl]-10,20-diphenylporphinato]zinc(II) Complexes. X-ray Crystal Structures of [5,15-Bis[(4′-fluorophenyl)ethynyl]-10,20-diphenylporphinato]zinc(II) and 5,15-Bis[(4′-methoxyphenyl)ethynyl]-10,20-diphenylporphyrin

Steven M. LeCours, Stephen G. DiMagno,‡ and Michael J. Therien*

Contribution from the Department of Chemistry, University of Pennsylvania, Philadelphia, Pennsylvania 19104-6323

Received July 12, 1996[⊗]

Abstract: A new class of porphyrins in which intervening ethynyl moieties connect aryl groups to the porphyrin 5- and 15-positions is described. The synthesis and optical spectroscopy of five new compounds are reported: [5,15-bis[(4′-dimethylaminophenyl)ethynyl]-10,20-diphenylporphinato]zinc(II), [5,15-bis[(4′-methoxyphenyl)ethynyl]-10,20-diphenylporphinato]zinc(II), [5,15-bis[(phenyl)ethynyl]-10,20-diphenylporphinato]zinc(II), [5,15-bis[(4′-fluorophenyl)-ethynyl]-10,20-diphenylporphinato]zinc(II), and [5,15-bis[(4′-nitrophenyl)ethynyl]-10,20-diphenylporphinato]zinc(II). The X-ray structure of one of these complexes, [5,15-bis[(4′-fluorophenyl)ethynyl]-10,20-diphenylporphinato]zinc(II), is unusual in that it shows the arylethynyl-phenyl rings to be coplanar with the porphyrin macrocycle. This arrangement of aryl rings with respect to the porphyrin macrocycle underscores the fact that the steric barrier to rotation between the porphyrin and arylethynyl-phenyl aromatic systems has been removed and highlights the enhanced π-conjugative interactions responsible for the unusual electronic characteristics of these molecules. Electronic spectroscopy and electrochemistry of these systems evince the ability of this new porphyrin structural motif to modulate extensively chromophore electronic structure. ZINDO-determined (INDO-1 semiempirical parameters; CI level = 20) frontier orbital energies for the [5,15-bis[(aryl)ethynyl]-10,20-diphenylporphinato]zinc(II) complexes demonstrate that these properties derive from energetic differences between the porphyrin HOMO and HOMO-1 and a substantial splitting of the formerly degenerate porphyrin LUMO; these significant electronic perturbations (relative to simple (porphinato)-zinc(II) complexes) are manifest in the fact that the low lying singlet excited states of these compounds are highly polarized.

Introduction

The ability to tune the electronic properties of porphyrins is crucial to catalyst design and for the precise control of the spectroscopic properties of photophysical probes, sensitizers, and the electron and energy transfer components of supramolecular systems.[1,2] The fact that there are twelve sites on the porphyrin (four *meso*- and eight β-positions) at which to attach electron-releasing or electron-withdrawing groups suggests that tremendous electronic modulation of the porphyrin ligand should be possible. Despite the fact that considerable control of porphyrin electronic properties has been accomplished, the scope of electronic modulation possible for a given porphyrin parent structure is limited. For example, a survey of the wide range of readily synthesized 5,10,15,20-tetrakis-(substituted-aryl)porphyrin ligands shows that (porphinato)metal spectral features are only moderately perturbed by aryl-group modification for a given metal ion, solvent, and axial ligand environment.[3] While single β-substitution of 5,10,15,20-tetra(aryl)porphyrins has a modest effect on the energies of the ligand valence orbitals,[4] tetra(*meso*-aryl)-porphyrin systems having highly-elaborated β-carbon positions exhibit considerably red-shifted electronic spectra;[5] however, since the optical and photophysical properties of such dodeca-substituted porphyrins derive from a combination of electronic effects and nonplanar distortions of the porphyrin ring, they often display surprisingly similar electronic and emission spectra, irrespective of whether their ring substituents are electron releasing or electron withdrawing.[6] Furthermore, many of the

‡ Address: Department of Chemistry, University of Nebraska-Lincoln, Lincoln, Nebraska 68588-0304.

⊗ Abstract published in *Advance ACS Abstracts,* November 1, 1996.

(1) (a) O'Neil, M. P.; Niemczyk, M. P.; Svec, W. A.; Gosztola, D.; Gaines, G. L., III; Wasielewski, M. R. *Science (Washington, D.C.)* **1992**, *257*, 63−65. (b) Gust, D.; Moore, T. A.; Moore, A. L.; *Acc. Chem. Res.* **1993**, *26*, 198−205. (c) Anderson, S.; Anderson, H. L.; Sanders, J. K. M. *Acc. Chem. Res.* **1993**, *26*, 469−475. (d) Sessler, J. L.; Capuano, V. L.; Harriman, A. *J. Am. Chem. Soc.* **1993**, *115*, 4618−4628. (e) Prathapan, S.; Johnson, T. E.; Lindsey, J. S. *J. Am. Chem. Soc.* **1993**, *115*, 7519−7520. (f) Ohkohchi, M.; Takahashi, A.; Mataga, N.; Okada, T.; Osuka, A.; Yamada, H.; Maruyama, K. *J. Am. Chem. Soc.* **1993**, *115*, 12137−12143. (g) Nishide, H.; Suzuki, T.; Nakagawa, R.; Tsuchida, E. *J. Am. Chem. Soc.* **1994**, *116*, 4503−4504.

(2) (a) Lin, V. S.-Y.; DiMagno, S. G.; Therien, M. J. *Science (Washington, D.C.)* **1994**, *264*, 1105−1111. (b) Angiolillo, P. J.; Lin, V. S.-Y.; Vanderkooi, J. M.; Therien, M. J. *J. Am. Chem. Soc.* **1995**, *117*, 12514−12527. (c) Lin, V. S.-Y.; Therien, M. J. *Chem. Eur. J.* **1995**, *1*, 645−651.

(3) (a) Kim, J. B.; Leonard, J. J.; Longo, F. R. *J. Am. Chem. Soc.* **1972**, *94*, 3986−3992. (b) Meot-Nor, M.; Adler, A. D. *J. Am. Chem. Soc.* **1975**, *97*, 5107−1511. (c) Quimby, D. J.; Longo, F. R. *J. Am. Chem. Soc.* **1975**, *97*, 5111−5117. (d) Spellane, P. J.; Gouterman, M.; Antipas, A.; Kim, S.; Liu, Y. C. *Inorg. Chem.* **1980**, *19*, 386−391. (e) McDermott, G. A.; Walker, F. A. *Inorg. Chim. Acta* **1984**, *91*, 95−102.

(4) Binstead, R. A.; Crossley, M. J.; Hush, N. S. *Inorg. Chem.* **1991**, *30*, 1259−1264.

S0002-7863(96)02403-1 CCC: $12.00

more electronically unusual porphyrins are substituted at the macrocycle periphery with elements beyond the first row of the periodic table;[3c,6−8] this generally results in deactivation of the porphyrin singlet excited state, a potential drawback if modulation of porphyrin photophysical properties is desired.

We report herein the utility of porphyrin-pendant *meso* arylethynyl moieties for extensively modulating the electronic properties of the porphyrin π system. This ability stems from the fact that the intervening ethynyl bridge assures a minimal steric barrier to rotation of the arylethynyl phenyl group with respect to the porphyrin core, thus providing enhanced conjugative interactions between their respective π symmetry orbitals.

Experimental Section

Materials. All manipulations were carried out under nitrogen previously passed through an O_2 scrubbing tower (Schweizerhall R3−11 catalyst) and a drying tower (Linde 3-Å molecular sieves) unless otherwise stated. Air-sensitive solids were handled in a Braun 150-M glove box. Standard Schlenk techniques were employed to manipulate air-sensitive solutions. All solvents utilized in this work were obtained from Fisher Scientific (HPLC Grade). Tetrahydrofuran (THF) was distilled from Na/benzophenone under N_2. Diethylamine was dried over KOH pellets and distilled under vacuum. All NMR solvents were used as received. 4-Iodoaniline, sodium cyanoborohydride, 4-iodoanisole, phenylacetylene, 1-fluoro-4-iodobenzene, 1-bromo-4-nitrobenzene, trimethylsilylacetylene, and ethynylmagnesium bromide were used as received (Aldrich). Formaldehyde solution (37% w/w) and anhydrous diethyl ether were used without further purification (Fisher), as was the $Pd[(PPh)_3]_4$ catalyst (Strem). 2,2′-Dipyrrylmethane was prepared according to the published procedure,[9] and stored under inert atmosphere at −40 °C. Chemical shifts for ^{1}H NMR spectra are relative to residual protium in the deuterated solvents ($CDCl_3$, $\delta = 7.24$ ppm; THF-d_8, $\delta = 3.58$ ppm). Chemical shifts for ^{13}C NMR spectra are relative to deuteriochloroform solvent ($CDCl_3$, $\delta = 77.00$ ppm). All J values are reported in Hertz. The number of attached protons is found in parentheses following the chemical shift value. Chromatographic purification (silica gel 60, 230−400 mesh, EM Science) of all newly synthesized 5,15-elaborated porphyrins was accomplished on the bench top. Elemental analyses were performed at Robertson Microlit Laboratories (Madison, NJ).

Instrumentation. Electronic spectra were recorded on an OLIS UV/vis/NIR spectrophotometry system that is based on the optics of a Cary 14 spectrophotometer. Cyclic and square wave voltammetric responses were recorded on an EG&G Princeton Applied Research Model 273A Potentiostat/Galvanostat.

Electronic Structure Calculations. Frontier orbital energies for the [5,15-bis[(aryl)ethynyl]-10,20-diphenylporphinato]zinc(II) complexes as well as the peripherally unsubstituted (porphinato)zinc(II) metallomacrocycle were determined utilizing CAChe ZINDO with standard INDO-1 semiempirical parameters at a configuration interaction (CI) level 20.[10] For all these complexes, the central zinc metal atoms were assigned a dsp^2 (square planar) geometry. (Porphinato)zinc(II) was constructed with D_{4h} symmetry while the [5,15-bis[(4′-X-phenyl)ethynyl]-10,20-diphenylporphinato]zinc(II) compounds were fashioned with either C_{2h} (X = NMe_2, OMe) or D_{2h} (X = H, F, NO_2) symmetries. All calculations were performed on ZINDO-optimized geometrical structures in which the dihedral angles of the 5- and 15-arylethynyl phenyl moieties with respect to the porphyrin least-squares plane were adjusted to 0°; the 10- and 20-*meso* phenyl groups were fixed at 90° with respect to the porphyrin plane. The convergence criteria for these Restricted Hartree-Fock (RHF) self-consistent field (SCF) calculations required the root mean square difference in the elements of the density matrix to be below 0.000 001 on two successive SCF cycles.

General Procedure for the Preparation of [5,15-Bis[(aryl)-ethynyl]-10,20-diphenylporphinato]zinc(II) Complexes. [5,15-dibromo-10,20-diphenylporphinato]Zn(II) (250 mg, 370 μmol), CuI (15 mg, 78 μmol), $Pd[PPh_3]_4$ (35 mg, 30 μmol), diethylamine (5 mL), THF (30 mL), and the desired phenylacetylene derivative (250 mg, ∼2 mmol) were brought together in a 100 mL Schlenk tube under an N_2 atmosphere. The resulting mixture turns green as the reaction proceeds at room temperature over 12−24 h. At the reaction endpoint, the crude product was purified by column chromatography on silica gel using 85:15 hexanes:THF as eluant. The green band was collected and evaporated to give an essentially pure [5,15-bis[(aryl)ethynyl]-10,20-diphenylporphinato]zinc(II) complex in high yield (> 85%). Recrystallization from THF/hexanes provided samples suitable for elemental analysis and X-ray crystallography.

[5,15-Bis[(4′-dimethylaminophenyl)ethynyl]-10,20-diphenylporphinato]zinc(II). Isolated yield = 62.3 mg (99%, based on 53.0 mg of the porphyrin starting material). Selected characterization data are as follows. ^{1}H NMR (250 MHz, 25:1 $CDCl_3$:pyridine-d_5): δ 9.63 (d, 4 H, J = 4.6), 8.75 (d, 4 H, J = 4.6), 8.10 (dd, 4 H, J_1= 7.5, J_2 = 2.9), 7.83 (d, 4 H, J = 8.6), 7.68 (m, 6 H), 6.80 (d, 4 H, J = 8.7), 3.02 (s, 12 H). ^{13}C NMR (60 MHz, 25:1 $CDCl_3$:pyridine-d_5): δ 151.65, 149.91, 149.35, 142.65, 135.47, 132.42, 131.83, 130.29, 126.97, 126.12, 118.60, 111.85, 111.28, 110.90, 97.46, 77.23, 40.00. Vis (THF): 466 (5.31), 675 (4.75). FAB MS: 810 (calcd 810). Anal. Calcd for $C_{52}H_{38}N_6Zn$: C, 76.89; H, 4.71; N, 10.35. Found: C, 76.63; H, 4.69; N, 10.37.

[5,15-Bis[(4′-methoxyphenyl)ethynyl]-10,20-diphenylporphinato]-zinc(II). Isolated yield = 285 mg (99%, based on 250 mg of the porphyrin starting material). Selected characterization data are as follows. ^{1}H NMR (500 MHz, 25:1 $CDCl_3$:pyridine-d_5): δ 9.78 (dd, 4 H, J_1= 4.2, J_2= 2.2), 8.89 (dd, 4 H, J_1= 4.4, J_2 = 1.4), 8.17 (d, 4 H, J = 6.4), 7.95 (d, 4 H, J = 8.5), 7.73 (m, 6 H), 7.06 (d, 4 H, J = 8.5), 3.84 (s, 6 H). ^{13}C NMR (60 MHz, 25:1 $CDCl_3$:pyridine-d_5): δ 159.57, 151.72, 149.69,142.60, 134.32, 132.81, 132.16, 130.43, 127.17, 126.26, 122.20, 116.32, 114.16, 101.17, 96.03, 77.20, 55.18. Vis (THF): 451 (5.60), 602 (4.05), 656 (4.79). FAB MS: 784 (calcd 784). Anal. Calcd for $C_{50}H_{32}N_4O_2Zn$: C, 76.39; H, 4.10; N, 7.13. Found: C, 76.04; H, 4.22; N, 7.01.

[5,15-Bis[(phenyl)ethynyl]-10,20-diphenylporphinato]zinc(II). Isolated yield = 47.5 mg (85%, based on 52.9 mg of the porphyrin starting material). Selected characterization data are as follows. ^{1}H NMR (250 MHz, 25:1 $CDCl_3$:pyridine-d_5): δ 9.67 (d, 4 H, J = 4.66), 8.81 (d, 4 H, J = 4.57), 8.12 (m, 4 H), 7.95 (d, 4 H, J = 6.87), 7.69 (m, 6 H), 7.45 (m, 6 H). ^{13}C NMR (60 MHz, 25:1 $CDCl_3$:pyridine-d_5): δ 151.81, 149.91, 134.39, 132.34, 131.39, 130.52, 128.54, 128.15, 127.27, 126.33, 124.22. Vis (THF): 446 (5.63), 593 (4.02), 650 (4.76). FAB MS: 724 (calcd 724). Anal. Calcd for $C_{50}H_{32}N_4O_2Zn$: C, 79.39; H, 3.89; N, 7.72. Found: C, 79.16; H, 3.86; N, 7.57.

(5) (a) Traylor, T. G.; Tsuchiya, S. *Inorg. Chem.* **1987**, *26*, 1338−1339. (b) Barkigia, K. M.; Berber, M. D.; Fajer, J.; Medforth, C. J.; Renner, M. W.; Smith, K. M. *J. Am. Chem. Soc.* **1990**, *112*, 8851−8857. (c) Bhyrappa, P.; Krishnan, V. *Inorg. Chem.* **1991**, *30*, 239−245. (d) Takeda, J.; Ohya, T.; Sato, M. *Chem. Phys. Lett.* **1991**, *183*, 384−386. (e) Wu, G.-Z.; Gan, W.-X.; Leung, H.-K. *J. Chem. Soc., Faraday Trans.* **1991**, *87*, 2933−2937. (f) Mandon, D.; Ochsenbein, P.; Fischer, J.; Weiss, R.; Jayaraj, K.; Austin, R. N.; Gold, A.; White, P. S.; Brigaud, O.; Battioni, P. Mansuy, D. *Inorg. Chem.* **1992**, *31*, 2044−2049. (g) Medforth, C. J.; Senge, M. O.; Smith, K. M.; Sparks, L. D.; Shelnutt, J. A. *J. Am. Chem. Soc.* **1992**, *114*, 9859−9869. (h) Lyons, J. E.; Ellis, P. E., Jr.; Wagner, R. W.; Thompson, P. B.; Gray, H. B.; Hughes, M. E.; Hodge, Jg. A. *Prepr.—Am. Chem. Soc., Div. Pet. Chem.* **1992**, *37*, 307−317. (i) Sparks, L. D.; Medforth, C. J.; Park, M.-S.; Chamberlain, J. R.; Ondrias, M. R.; Senge, M. O.; Smith, K. M.; Shelnutt, J. A. *J. Am. Chem. Soc.* **1993**, *115*, 581−592. (j) Senge, M. O.; Medforth, C. J.; Sparks, L. D.; Shelnutt, J. A.; Smith, K. M. *Inorg. Chem.* **1993**, *32*, 1716−1723.

(6) A comparison of the Soret absorption wavelengths in a series of substituted (porphinato)nickel complexes (solvent = CH_2Cl_2) shows the following: (5,10,15,20-tetraphenylporphinato)Ni(II) (λ = 414 nm); (5,10,15,20-tetraphenyl-2,3,7,8,12,13,17,18-octamethylporphinato)Ni(II) (λ = 418 nm); (5,10,15,20-tetraperfluorophenyl-2,3,7,8,12,13,17,18-octabromoporphinato)Ni(II) (λ = 436 nm); (5,10,15,20-tetraphenyl-2,3,7,8,12,13,17,18-octabromoporphinato)Ni(II) (λ = 448 nm); (2,3,5,7,8,10,12,13,15,17,18,20-dodecaphenylporphinato)Ni(II) (λ = 448 nm). See refs 5b, e, f, and g.

(7) Gouterman, M. In *The Porphyrins*, Dolphin, D., Ed.; Academic Press, London, 1978; Vol. III, pp 1−165.

(8) Bonnett, R.; Harriman, A.; Kozyrev, A. N. *J. Chem. Soc., Faraday Trans.* **1992**, *88*, 763−769.

(9) Chong, R.; Clezy, P. S.; Liepa, A. J.; Nichol, A. W. *Aust. J. Chem.* **1969**, *22*, 229−238.

(10) ZINDO Software provided by CAChe Scientific, Beaverton, OR.

Table 1. Summary of Structure Determination of [5,15-Bis(4′-fluorophenylethynyl)-10,20-diphenylporphinato]zinc(II) and 5,15-Bis(4′-methoxyphenyl)-10,20-diphenylporphyrin

formula	$C_{48}H_{26}N_4F_2Zn\cdot2(C_4H_8O)$	$C_{50}H_{32}N_4O_2\cdot2(CHCl_3)$
formula weight	906.35	961.61
crystal class	hexagonal	triclinic
space group	$R\bar{3}$ (no. 148)	$P\bar{1}$ (no. 2)
Z	9	1
cell constants		
a	28.595(2) Å	10.352(3) Å
b	14.980(4) Å	10.975(2) Å
c	14.980(4) Å	11.694(2) Å
α		78.51(2)°
β		107.14(2)°
γ		113.92(2)°
V	10608(5) Å^3	1156(1) Å^3
μ	5.84 cm^{-1}	38.26 cm^{-1}
crystal size, mm	0.32 × 0.45 × 0.50	0.08 × 0.40 × 0.42
trans. (min, max, av, %)	95.73, 99.97, 99.03	
D_{calc}	1.277 g/cm^3	1.381 g/cm^3
F(000)	4230	494
radiation	Mo-Kα (λ = 0.710 73 Å)	Cu-Kα (λ = 1.541 84 Å)
θ range	2.0−25.0	2.0−65.0
scan mode	ω-2θ	ω-2θ
h,k,l collected	+18, +18, ±20	−12, ±12, ±13
no. reflcns measured	5144	4177
no. unique reflcns	4140	3938
no. reflcns used in refinement	3045 ($F^2 > 3.0\sigma$)	2538 ($F^2 > 3.0\sigma$)
no. parameters	295	289
data/parameter ratio	10.3	8.8
R_1	0.057	0.088
R_2	0.086	0.114
GOF	0.974	3.247

[5,15-Bis[(4′-fluorophenyl)ethynyl]-10,20-diphenylporphinato]-zinc(II). Isolated yield = 64.9 mg (93%, based on 62.9 mg of the porphyrin starting material). Selected characterization data are as follows. ^{1}H NMR (250 MHz, $CDCl_3$,): δ 9.66 (d, 4 H, J = 4.6), 8.83 (d, 4 H, J = 4.6), 8.16 (dd, 4 H, J_1= 7.1, J_2= 2.1), 7.96 (td, 4 H, J_1= 7.1, J_2= 3.2), 7.75 (m, 6 H), 7.22 (t, 4 H, J = 8.7). ^{13}C NMR (60 MHz, 25:1 $CDCl_3$:pyridine-d_5): δ 171.34 (d, 2 C, J = 275), 151.74, 149.91, 142.50, 134.35, 133.21 (d, 4 C, J = 7.5), 132.38, 130.46, 127.27, 126.33, 122.5, 115.80 (d, 4 C, J = 21.9), 100.54, 94.84, 92.80, 77.2. Vis (THF): 446 (5.57), 592 (4.02), 648 (4.70). FAB MS: 760 (calcd 760). Anal. Calcd for $C_{48}H_{26}N_4F_2Zn$: C, 75.65; H, 3.44; N, 7.35. Found: C, 75.39; H, 3.31; N, 7.32.

[5,15-Bis[(4′-nitrophenyl)ethynyl]-10,20-diphenylporphinato]-zinc(II). Isolated yield = 205 mg (93%, based on 184.5 mg of the porphyrin starting material). Selected characterization data are as follows. ^{1}H NMR (500 MHz, pyridine-d_5): δ 9.67 (d, 4 H, J = 4.5), 8.91 (d, 4 H, J = 4.5), 8.27 (d, 4 H, J = 8.5), 8.16 (d, 4 H, J = 6.4), 7.97 (d, 4 H, J = 8.6), 7.75 (m, 6 H). ^{13}C NMR (125 MHz, pyridine-d_5): δ 148.91, 134.49, 133.68, 132.32, 131.16, 130.21, 126.91, 125.89, 123.07. Vis (THF): 460 (5.45), 666 (4.82). Anal. Calcd for $C_{48}H_{26}N_6O_4Zn$: C, 70.64; H, 3.21; N, 10.30. Found: C, 70.37; H, 3.27; N, 10.14.

X-ray Crystallography.[11] The crystal structures for [5,15-bis[(4′-fluorophenyl)ethynyl]-10,20-diphenylporphinato]zinc(II) and [5,15-bis-[(4′-methoxyphenyl)ethynyl]-10,20-diphenylporphyrin were solved by direct methods (SIR88).[12] Table 1 contains details of the crystal and data collection parameters. The structures were determined by Dr. Patrick Carroll at the Chemistry Department's X-ray facility at the University of Pennsylvania.

[5,15-Bis[(4′-fluorophenyl)ethynyl]-10,20-diphenylporphinato]-zinc(II). Crystallization was induced by layering hexane onto a saturated THF solution of the compound; storing the mixture at 0 °C under N_2 for 3 days gave rectangular purple prisms. The crystal dimensions were 0.32 × 0.45 × 0.50 mm^3. [5,15-Bis[(4′-fluorophenyl)-ethynyl]-10,20-diphenylporphinato]zinc(II) crystallizes in the hexagonal space group $R\bar{3}$ with a = 28.595(2) Å, b = c = 14.980(4) Å, V = 10608(9) Å^3, Z = 9, and d_{calc} = 1.277 g cm^{-3}. The cell constants were determined from a least-squares fit of the setting angles for 25 accurately centered reflections. X-ray intensity data were collected on an Enraf-Nonius CAD4 diffractometer employing graphite-monochromated Mo-Kα radiation (λ = 0.710 73 Å) and using the ω-2θ scan technique. A total of 5144 reflections were measured over the ranges: $4 \le 2\theta \le 50°$, $0 \le h \le 18$, $0 \le k \le 18$, $-20 \le l \le 20$. Three standard reflections measured every 3500 s of X-ray exposure showed an intensity decay 15.1% over the course of the data collection.

The intensity data were corrected for Lorentz and polarization effects and an empirical absorption correction was applied (minimum transmission 95.73%, max 99.97%, mean 99.03%). Of the reflections measured, a total of 3045 unique reflections with $F^2 > 3\sigma(F^2)$ were used during subsequent structure refinement.

Refinement was by full-matrix least squares techniques based on F to minimize the quantity $\sum w(|F_o| - |F_c|)^2$ with $w = 1/\sigma^2(F)$. Non-hydrogen atoms were refined anisotropically and hydrogen atoms were included as constant contributions to the structure factors and were not refined. Refinement converged to R_1 = 0.057 and R_2 = 0.086.

[5,15-Bis[(4′-methoxyphenyl)ethynyl]-10,20-diphenylpor-phyrin. Crystallization was induced by dissolving the compound in $CHCl_3$ and storing the crystallization vessel at −40 °C overnight to give purple plates. The crystal dimensions were 0.08 × 0.40 × 0.42 mm^3. [5,15-Bis[(4′-methoxyphenyl)ethynyl]-10,20-diphenylporphyrin crystallizes in the triclinic space group $P\bar{1}$ with a = 10.352(3) Å, b = 10.975(2)Å, c = 11.694(2) Å, a = 78.51°, b = 107.14(2)°, c = 113.92(2)°, V = 1156(1) Å^3, Z = 1 and d_{calc} = 1.381 g cm^{-3}. The cell constants were determined from a least squares fit of the setting angles for 25 accurately centered reflections. A total of 4177 reflections were measured over the ranges: $4 \le 2\theta \le 130°$, $-12 \le h \le 0$, $-12 \le k \le 12$, $-13 \le l \le 13$. Three standard reflections measured every 3500 s of X-ray exposure showed an intensity decay of 17.7% over the course of the data collection. A linear decay correction was applied.

The intensity data were corrected for Lorentz and polarization effects, and an empirical absorption correction was (DIFABS) was performed. Of the reflections measured, a total of 2538 unique reflections with $F^2 > 3\sigma(F^2)$ were used during subsequent structure refinement.

Refinement was by full-matrix least squares techniques based on F to minimize the quantity $\sum w(|F_o| - |F_c|)^2$ with $w = 1/\sigma^2(F)$. Non-

(11) The atomic coordinates for these structures have been deposited with the Cambridge Crystallographic Data Centre. The coordinates can be obtained, on request, from the Director, Cambridge Crystallographic Data Centre, 12 Union Road, Cambridge, CB2 1EZ UK.

(12) Burla, M. C.; Camalli, M.; Cascarano, G.; Giacovazzo, C.; Polidori, G.; Spagna, R.; Viterbo, D. *J. Appl. Crystallogr.* **1989**, *72*, 389−93.

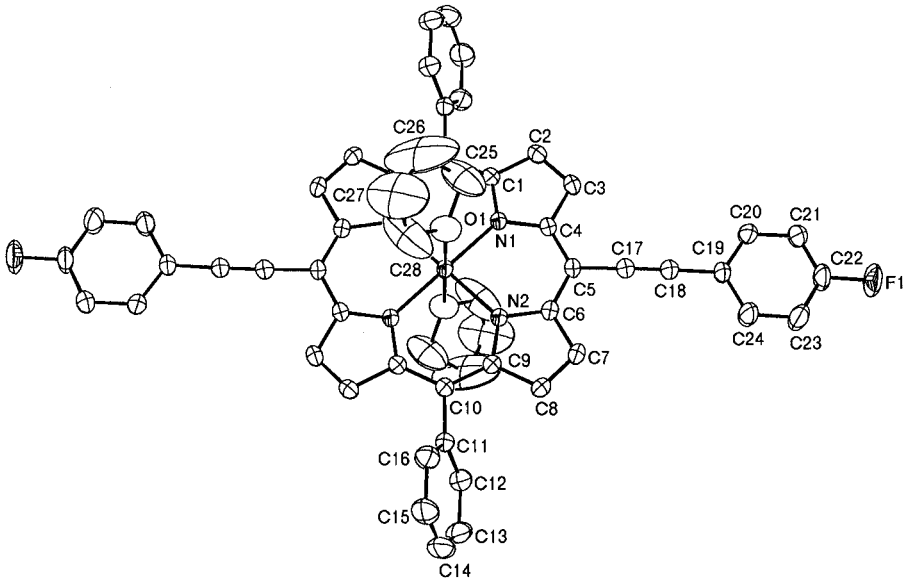

Figure 1. ORTEP view of [5,15-bis[(4′-fluorophenyl)ethynyl]-10,20-diphenylporphinato]zinc(II) with thermal ellipsoids at 30% probability.

hydrogen atoms were refined anisotropically and hydrogen atoms were included as constant contributions to the structure factors and were not refined. Refinement converged to $R_1 = 0.088$ and $R_2 = 0.114$.

Results and Discussion

Synthesis, Solution Properties, and Structural Studies. In 5,10,15,20-tetrakis(substituted-aryl)porphyrins, steric crowding from the interaction of the phenyl *ortho* protons with the porphyrin β-hydrogens results in a large dihedral angle between the planes of the rings, thereby limiting porphyrin electronic tuning via π-conjugative interactions. In an effort to prepare structurally simple porphyrins with unusual electronic characteristics, we have sought to remove this steric barrier between the two aromatic systems; this has been accomplished through the utility of an intervening acetylenyl moiety which serves as a cylindrically π-symmetric interconnect between the phenyl and porphyryl rings.

A series of [5,15-bis[(4′-substituted-phenyl)ethynyl]-10,20-diphenylporphinato]zinc(II) complexes that included [5,15-bis-[(4′-dimethylaminophenyl)ethynyl]-10,20-diphenylporphinato]-zinc(II), [5,15-bis[(4′-methoxyphenyl)ethynyl]-10,20-diphenyl-porphinato]zinc(II), [5,15-bis[(phenyl)ethynyl]-10,20-diphenylporphinato]zinc(II), [5,15-bis[(4′-fluorophenyl)ethynyl]-10,20-diphenylporphinato]zinc(II), and [5,15-bis[(4′-nitrophenyl)-ethynyl]-10,20-diphenylporphinato]zinc(II) were synthesized in high yield (> 85%) through metal-mediated cross-coupling of the substituted arylethynyl groups[13] to [5,15-dibromo-10,20-diphenylporphinato]zinc(II).[2,14] An X-ray crystallographic structure was determined for one of these compounds, the bis(THF) adduct of [5,15-bis[(4′-fluorophenyl)ethynyl]-10,20-diphenylporphinato]zinc(II); an ORTEP view of this complex is shown in Figure 1. Of particular importance are the following: (i) While the 10,20-aryl groups show a typical orientation with respect to the porphyrin ring (dihedral angle = 79.7°), the arylethynyl phenyl rings and the porphyrin macrocycle adopt a nearly coplanar arrangement with a dihedral angle of 4.3°. (ii) The carbon-carbon triple bond length is 1.19 Å, and hence, is unexceptional. (iii) The bond lengths observed in the porphyrin framework resemble those observed in Schauer's crystal structure of [5,10,15,20-tetraphenylporphinato]zinc(II).[15] Since these latter points indicate that there is no cumulenic character at the acetylenic- or *meso*-carbon atoms, the near coplanarity of the arylethynyl moiety with the porphyrin unit in the solid state may derive in large part from crystal packing forces.

The free base derivatives of these complexes can be prepared from their (porphinato)zinc(II) precursors using standard experimental conditions; straightforward remetalation of such 5,15-bis[(aryl)ethynyl]-10,20-diphenylporphyrin compounds provides an entry into other [5,15-bis[(aryl)ethynyl]-10,20-diphenylporphinato]metal complexes.[16] In contrast to the [5,15-bis[(aryl)-ethynyl]-10,20-diphenylporphinato]zinc(II) compounds, which are appreciably soluble in coordinating solvents such as THF and pyridine, as well as polar solvents such as CH_2Cl_2 and benzonitrile that have small amounts of added pyridine, the free ligand derivatives are less soluble, with ~0.1−1 mM solutions saturating $CHCl_3$ and aromatic solvents (benzene, toluene, benzonitrile).

The results of our single-crystal X-ray crystallographic study of a 5,15-bis[(4′-methoxyphenyl)ethynyl]-10,20-diphenylporphyrin are shown in Figure 2; note that this ORTEP diagram emphasizes many features in common with the [5,15-bis[(4′-fluorophenyl)ethynyl]-10,20-diphenylporphinato]zinc(II)·$(THF)_2$ structure. Table 2 compiles selected bond lengths and bond angles for these two compounds.

The porphyrin cores for both 5,15-bis[(4′-methoxyphenyl)-ethynyl]-10,20-diphenylporphyrin and [5,15-bis[(4′-fluoro-phenyl)ethynyl]-10,20-diphenylporphinato]zinc(II)·$(THF)_2$ are flat, as indicated by the fact that the maximal deviation of any atom from the porphyrin least squares plane is 0.04 Å and 0.05 Å, in these two respective structures. The $C(5)_{meso}$-to-$C\alpha_{(ethynyl)}$, $C\alpha_{(ethynyl)}$-to-$C\beta_{(ethynyl)}$, and $C\beta_{(ethynyl)}$-to-$C(1')_{(phenyl)}$ bond lengths in 5,15-bis[(4′-methoxyphenyl)ethynyl]-10,20-diphenylporphyrin are similar to that observed for [5,15-bis[(4′-fluoro-phenyl)ethynyl]-10,20-diphenylporphinato]zinc(II)·$(THF)_2$ (1.437, 1.187, and 1.432 Å, respectively) and likewise signal no ground-

(13) (a) Eastmond, R.; Walton, D. R. M. *Tetrahedron* **1972**, *28*, 4591−4599. (b) Westmijze, H.; Vermeer, P. *Synthesis* **1979**, 390−392. (c) Takahashi, S.; Kuroyama, Y.; Sonogashira, K.; Hagihara, N. *Synthesis* **1980**, 627−630. (d) Mesnard, D.; Bernadou, F.; Miginiac, L. *J. Chem. Res. (S)* **1981**, 270−271. (e) Zhang, Y.; Wen, J. *Synthesis* **1990**, 727−728. (f) Park, K. M.; Schuster, G. B. *J. Org. Chem.* **1992**, *57*, 2502−2504.

(14) (a) DiMagno, S. G.; Lin, V. S.-Y.; Therien, M. J. *J. Am Chem. Soc.* **1993**, *115*, 2513−2515. (b) DiMagno, S. G.; Lin, V. S.-Y.; Therien, M. J. *J. Org. Chem.* **1993**, *58*, 5983−5993.

(15) Schauer, C. K.; Anderson, O. P.; Eaton, S. S.; Eaton, G. R. *Inorg. Chem.* **1985**, *24*, 4082−4086.

(16) LeCours, S. M.; Therien, M. J. Manuscript in preparation.

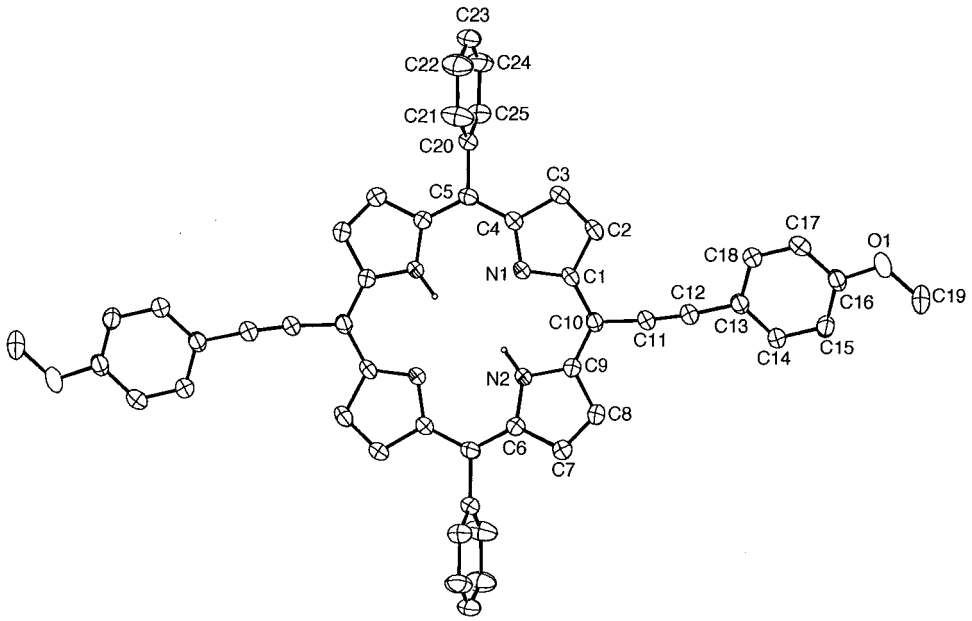

Figure 2. ORTEP view of 5,15-bis[(4′-methoxyphenyl)ethynyl]-10,20-diphenylporphyrin with thermal ellipsoids at 30% probability.

state cumulenic character along the vector connecting the porphyrin C(5)$_{meso}$ and the arylethynyl phenyl C(1′) carbon atoms.

There are measurable differences between the two structures in their respective C(5)$_{meso}$-C$\alpha_{(ethynyl)}$-C$\beta_{(ethynyl)}$ bond angles: this angle is 174.4(5) in the 5,15-bis[(4′-methoxyphenyl)ethynyl]-10,20-diphenylporphyrin structure and 178.3(4) for that of [5,15-bis[(4′-fluorophenyl)ethynyl]-10,20-diphenylporphinato]-zinc(II)·(THF)$_2$. It is interesting to note that the magnitudes of the C(5)$_{meso}$-C$\alpha_{(ethynyl)}$-C$\beta_{(ethynyl)}$ angles parallel those observed for C$\alpha_{(ethynyl)}$-C$\beta_{(ethynyl)}$-C(1′)$_{(phenyl)}$ in these two structures. Because there is no obvious electronic genesis for this difference in topology about the ethyne unit in these two compounds, these variances may derive from dissimilar crystal packing forces for these (porphinato)zinc(II) and porphyrin compounds; congruent with this notion, the arylethynyl phenyl rings and the porphyrin macrocycle are not as coplanar in the 5,15-bis[(4′-methoxyphenyl)ethynyl]-10,20-diphenylporphyrin (dihedral angle = 16.6° between the two aromatic systems) as they are in the [5,15-bis[(4′-fluorophenyl)ethynyl]-10,20-diphenylporphinato]-zinc(II))·(THF)$_2$ structure (*vide supra*). If dissimilar crystal packing forces are indeed responsible for these structural differences, a possible origin could lie in the fact that two chloroform molecules pack closely about each ethyne unit in 5,15-bis[(4′-methoxyphenyl)ethynyl]-10,20-diphenylporphyrin (data not shown); three intermolecular contacts are made between the porphyrin ligand and solvent that are close to the sum of the Cl-H van der Waals radius of 2.95 Å.

Electrochemical Studies. To probe for evidence of ground-state electronic communication between the arylethynyl-phenyl rings and the porphyrin macrocycle, we examined the cathodic and anodic electrochemistry of the [5,15-bis[(4′-X-phenyl)-ethynyl]-10,20-diphenylporphinato]zinc(II) complexes. Figure 3A shows the cyclic voltammetric response obtained for a benzonitrile solution of [5,15-bis[(4′-methoxyphenyl)ethynyl]-10,20-diphenylporphinato]zinc(II) while Figure 3B shows the observable redox couples for [5,15-bis[(phenyl)ethynyl]-10,20-diphenylporphinato]zinc(II) recorded in THF. Due to the magnitude of the potentiometric window defined by the ZnP^+/ZnP^{2+} and ZnP^-/ZnP^{2-} redox couples for this series of compounds, no single solvent was suitable for examining all four redox processes that characterize their oxidative and reductive electrochemistry.

Table 3 summarizes the anodic cyclic voltammetric data for these[5,15-bis[(4′-X-phenyl)ethynyl]-10,20-diphenylporphinato]-zinc(II) species in benzonitrile solvent.[17] The marginal solubility of the X = NO_2 and X = NMe_2 derivatives in both CH_2Cl_2 and benzonitrile precluded a comprehensive evaluation of the effect of the 4′-X substituent on the ZnP/ZnP^+ and ZnP^+/ZnP^{2+} potentials in the absence of the inherent experimental and data-analysis complications that arise if exogenous coordinating ligands are added to the solvent. Nevertheless, a clear trend is discernible in the ZnP/ZnP^+ redox potentials, which shows that the $E_{1/2}$ values of X = OMe, H, and F derivatives extend over a 118 mV range and track with substituent electronic properties. These data are *remarkable* in that they demonstrate that these electron releasing and withdrawing groups impact the stability of the chromophore HOMO despite the fact that they lie at remote distances from the porphyrin core. It is worth noting in this regard that 2-bromo-5,10,15,20-tetraphenylporphyrin (2-BrTPP) possesses an oxidation potential only 80 mV more positive than TPP,[18] and that the series of compounds [5,10,-15,20-tetraphenylporphinato]copper(II) (TPPCu), 2-OMeTPPCu, and 2-ClTPPCu, exhibit ring-centered first oxidation potentials that span only a 102 mV regime.[4]

A comprehensive cathodic cyclic voltammetric data set can be obtained for the [5,15-bis[(4′-X-phenyl)ethynyl]-10,20-diphenylporphinato]zinc(II) complexes in THF solvent (Table 4). Consistent with the data shown in Table 3, the entries in Table 4 underscore the conclusion that the 4′-X substituents can indeed modulate the stability of the (porphinato)zinc(II) frontier orbitals to a significant degree; note that the first cathodic reduction wave (E_{pc}) for these complexes varies from −1333 mV for the X = NMe_2 derivative to −1088 mV for the X = NO_2 complex, spanning a 245 mV potential domain. As was observed for the ZnP^+/ZnP^{2+} potentials with respect to their respective ZnP/ZnP^+ redox processes, the complexes that exhibit

(17) Electrochemical studies carried out in benzonitrile were performed on analytically pure (porphinato)zinc(II) compounds. Note that the [5,15-bis[(4′-X-phenyl)ethynyl]-10,20-diphenylporphinato]zinc(II) complexes (X = NO_2, F, OMe, and NMe_2) reported in this study analyze as their axial-ligand free derivatives (see Experimental Section). In general, if dried under vacuum for 24 h at 120 °C, these compounds are isolated free of axial THF ligands; if simply recrystallized from THF, they are isolated as their bis(THF) adducts.

(18) Giraudeau, A.; Callot, H. J.; Gross, M. *Inorg. Chem.* **1979**, *18*, 201−206.

Table 2. Selected Bond Distances and Angles

bond	distance, Å	angle	angle, deg
	5,15-Bis(4′-methoxy-phenylethynyl)-10,20-diphenylporphyrin		
C1−C2	1.444(6)	C2−C1−C10	123.8(4)
C1−C10	1.410(6)	C2−C1−N1	110.1(3)
C1−N1	1.354(5)	C10−C1−N1	126.0(4)
C2−C3	1.349(6)	C1−C2−C3	106.9(4)
C3−C4	1.445(7)	C2−C3−C4	106.3(4)
C4−C5	1.412(6)	C3−C4−C5	123.2(4)
C4−N1	1.361(5)	C3−C4−N1	110.2(4)
C5−C20	1.503(6)	C5−C4−N1	126.6(4)
C6−C7	1.418(6)	C4−C5−C20	117.5(4)
C6−N2	1.360(5)	C7−C6−N2	107.7(4)
C7−C8	1.345(7)	C6−C7−C8	108.0(4)
C8−C9	1.435(6)	C7−C8−C9	107.7(4)
C9−C10	1.398(6)	C8−C9−C10	125.9(4)
C9−N2	1.358(6)	C8−C9−N2	107.2(4)
C10−C11	1.435(6)	C10−C9−N2	127.0(4)
C11−C12	1.185(6)	C1−C10−C9	125.3(4)
C12−C13	1.434(6)	C1−C10−C11	116.4(4)
C13−C14	1.392(7)	C9−C10−C11	118.3(4)
C14−C15	1.384(7)	C10−C11−C12	174.4(5)
C15−C16	1.397(7)	C11−C12−C13	175.5(5)
C16−O1	1.353(6)	C12−C13−C14	122.5(4)
C19−O1	1.396(6)	C12−C13−C18	119.4(4)
C20−C21	1.381(9)	C14−C13−C18	118.1(4)
C21−C22	1.383(8)	C21−C20−C25	117.2(5)
C22−C23	1.357(10)	C1−N1−C4	106.4(3)
		C6−N2−C19	109.4(3)
		C10−O1−C19	118.5(4)
	[5,15-Bis(4′-fluorophenylethynyl)-10,20-diphenylporphinato]zinc(II)		
Zn−O1	2.429(5)	N1−Zn−N2	90.5(2)
F1−C22	1.366(9)	Zn−N1−C1	127.0(4)
N1−C1	1.362(7)	N1−C1−C1	109.2(5)
C2−C3	1.332(9)	C1−C2−C3	107.0(5)
C10−C11	1.498(7)	N1−C4−C5	125.5(5)
C19−C20	1.378(8)	C4−C5−C17	117.5(5)
C21−C22	1.353(10)	C8−C9−C10	125.1(5)
C20−C21	1.367(10)	C9−C10−C11	117.1(5)
Zn−N1	2.053(4)	C5−C17−C18	178.3(4)
N1−C4	1.360(7)	C1−N1−C4	106.8(4)
C1−C2	1.439(8)	N1−C4−C3	109.4(5)
C3−C4	1.431(7)	N2−C9−C10	125.8(5)
C4−C5	1.402(8)	C19−C20−C21	121.1(6)
C5−C17	1.439(9)	O1−Zn−N1	91.0(2)
C9−C10	1.400(8)	Zn−N1−C4	126.1(3)
C17−C18	1.189(9)	Zn−N2−C9	126.8(4)
C18−C19	1.430(9)	C2−C3−C4	107.6(5)
		C3−C4−C5	125.1(5)
		C10−C11−C12	120.5(5)
		C17−C18−C19	178.8(5)
		C20−C19−C24	118.4(6)
		F1−C22−C21	119.2(5)
		C4−C5−C6	126.6(5)
		C18−C19−C20	120.8(6)

chemically reversible ZnP/ZnP$^-$ redox couples show considerable leveling of the effect of the 4′-X substituents on their corresponding ZnP$^-$/ZnP^{2-} $E_{1/2}$ values (Tables 3 and 4).

Optical Spectra of [5,15-Bis[(4′-X-phenyl)ethynyl]-10,20-diphenylporphinato]zinc(II) Complexes. The electronic spectra of the [5,15-bis[(4′-X-phenyl)ethynyl]-10,20-diphenylporphinato]zinc(II) complexes shown in Figure 4 display a number of interesting characteristics; Table 5 highlights the prominent visible region spectral signatures of these complexes. In contrast to the electronic spectrum of [5,15-bis(trimethysilylethynyl)-10,20-diphenylporphinato]zinc(II),[2a] which shows a Soret (B) band split into discernible B_x and B_y transitions, the optical spectra of the [5,15-bis[(aryl)ethynyl]-10,20-diphenylporphinato]-zinc(II) complexes show a single broad B band (FWHM = 753 - 1157 cm^{-1}; Table 5). Apparently, the addition of the auxiliary conjugated groups to the ethynes further diminishes the relative intensity of the B_y transition;[2a,c] the lion's share of the observed B band's oscillator strength thus corresponds to a transition considerably polarized along the C_2 (x) axis defined by the arylethynyl groups.

Another consequence of removing the degeneracy of the porphyrin e_g symmetry LUMO through the attachment of arylethynyl moieties to the porphyrin *meso* position is manifest in the Q band region of the spectrum; here the lowest energy π-π^* transition features an extinction coefficient of approximately 60 000 M^{-1} cm^{-1}, displaying significantly enhanced oscillator strength (Table 5) with respect to tetra(*meso*-aryl)-

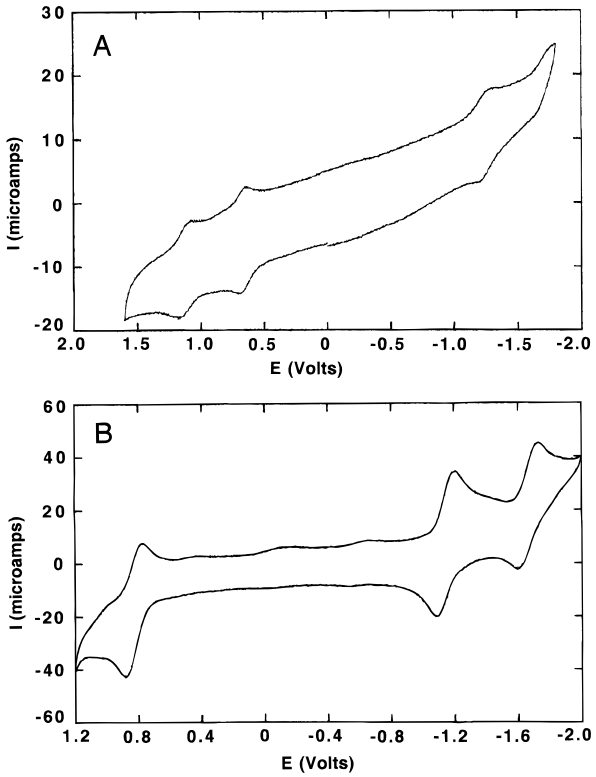

Figure 3. (A) Cyclic voltammogram of [5,15-bis[(4′-methoxyphenyl)-ethynyl]-10,20-diphenylporphinato]zinc(II) recorded in benzonitrile solvent showing the two anodic redox couples (ZnP/ZnP$^+$ and ZnP$^+$/ZnP^{2+}) as well as the initial cathodic redox process (ZnP/ZnP$^-$). (B) Cyclic voltammogram of [5,15-bis[(phenyl)ethynyl]-10,20-diphenylporphinato]zinc(II) recorded in THF solvent showing the two cathodic redox couples (ZnP/ZnP$^-$ and ZnP$^-$/ZnP^{2-}) as well as the initial anodic redox process (ZnP/ZnP$^+$). Cyclic voltammetric experimental conditions are described in Tables 3 and 4, respectively.

Table 3. Oxidative Cyclic Voltammetric Data[a] for [5,15-Bis[(4′-X-aryl)ethynyl]-10,20-diphenylporphinato]zinc(II) Compounds Recorded in Benzonitrile Solvent

	ZnP/ZnP$^+$				ZnP$^+$/ZnP^{2+}			
compd	E_{pa} (mV)	E_{pc} (mV)	$E_{1/2}$ (mV)	ΔE_p (mV)	E_{pa} (mV)	E_{pc} (mV)	$E_{1/2}$ (mV)	ΔE_p (mV)
X = NMe$_2$[b]								
X = OMe	662	599	630	63	1122	1022	1072	100
X = H	745	690	718	55	1242	1112	1177	130
X = F	780	715	748	65	1222	1105	1164	117
X = NO$_2$[b]								

[a] Cyclic voltammetric experimental conditions: [Porphyrin] = 1−3 mM; [TBAPF$_6$] = 0.15 M; scan rate = 200 mV/s; reference electrode = saturated calomel (SCE); working electrode = platinum disk; the ferrocene/ferrocenium (Fe^{II}/Fe^{III}) redox couple (0.43 V vs SCE) was used as an internal standard. The experimental uncertainty in these reported potentials is ±3 mV. [b] Very low solubility of these complexes in benzonitrile and CH_2Cl_2 precluded investigation of the anodic electrochemistry of these complexes.

Table 4. Reductive Cyclic Voltammetric Data[a] for [5,15-Bis[(4′-X-phenyl)ethynyl]-10,20-diphenylporphinato]zinc(II) Compounds Recorded in THF Solvent

	ZnP/ZnP$^-$				ZnP$^-$/ZnP^{2-}			
compd	E_{pc} (mV)	E_{pa} (mV)	$E_{1/2}$ (mV)	ΔE_p (mV)	E_{pc} (mV)	E_{pa} (mV)	$E_{1/2}$ (mV)	ΔE_p (mV)
X = NMe_2	−1333	−1246	−1290	87	−1818	−1703	−1760	115
X = OMe	−1253	−1168	−1210	85	−1783	−1608	−1696	175
X = H	−1303	−1188	−1246	115	−1820	−1710	−1765	110
X = F	−1218	−1163	−1190	55	−1843	−1693	−1768	150
X = NO2	−1088[b]				−1361[c]	−1198[c]	−1280[c]	163[c]

[a] Cyclic voltammetric experimental conditions: [Porphyrin] = 1−3 mM; [$TBAPF_6$] = 0.15 M; scan rate = 200 mV/s; reference electrode = saturated calomel (SCE); working electrode = platinum disk; the ferrocene/ferrocenium (Fe^{II}/Fe^{III}) redox couple (0.43 V vs SCE) was used as an internal standard. The experimental uncertainty in these reported potentials is ±3 mV. [b] The first electrode-coupled is irreversible and displays a cyclic voltammetric response consistent with an EC process. Noticeable fouling of the electrode surface was apparent after this initial reduction event irrespective of scan rate. [c] The nature of the second cathodic redox process exhibited by 5,15-bis[(4′-nitrophenyl)ethynyl]-10,20-diphenylporphinato]zinc(II) is undetermined.

Table 5. Comparative Integrated Oscillator Strengths and Absorptive Domains of the Blue and Red Spectral Regions of [5,15-Bis[(4′-X-phenyl)ethynyl]-10,20-diphenylporphinato]zinc(II) Complexes in THF Solvent

compd	FWHM[a] B-band region [cm^{-1}, (nm)]	oscillator strength B-band region[c]	FWHM[b,d] Q-band region [cm^{-1}, (nm)]	oscillator strength Q-band region[e]	oscillator strength (360 → 750 nm)
X = NMe_2	1157 (466)	1.29	888 (676)	0.244	1.54
X = OMe	789 (451)	1.59	660 (656)	0.213	1.80
X = H	753 (446)	1.65	598 (650)	0.200	1.85
X = F	779 (446)	1.42	587 (648)	0.171	1.59
X = NO_2	976 (460)	1.52	749 (666)	0.251	1.77

[a] Taken as the spectral width of the B-band region at half the height of λ_{max}. [b] Entries correspond to the spectral window centered about the electronic transition in parentheses. [c] Oscillator strengths calculated over the (360 → 530 nm) wavelength domain. [d] Taken as the spectral width of the Q-band region at half the height of λ_{max}. [e] Oscillator strengths calculated over the (530 → 750 nm) wavelength domain.

porphyrins, twice that observed for the $Q_{(0,0)}$ absorption of [5,10,15,20-tetraphenylporphinato]zinc(II).[2c] The intense, low energy Q bands of [5,15-bis[(4′-X-phenyl)ethynyl]-10,20-diphenylporphinato]zinc(II) species are on average 620 cm^{-1} more red shifted than the analogous transition observed for [5,15-bis(trimethysilylethynyl)-10,20-diphenylporphinato]zinc(II),[2a] and exhibit extinction coefficients three times as great. Both theory and experiment show that when porphyrin ring substituents enhance the splitting between the key filled (a_{1u}, a_{2u}) or empty (e_g) orbitals in simple 4-fold symmetric porphyrins, the Q transition gains in intensity; intensity enhancements of the type shown in Figure 2, however, are unprecedented for simple *meso*-substituted porphyrins.[3d,7,19] A weaker transition ($\epsilon \sim 10\,000$ M^{-1} cm^{-1}), slightly higher in energy with respect to the λ_{max} of the lowest energy Q-type transition is observed for these species; in Figure 4, this absorption is clearly discernible for the 4′-X = F, H, and OMe [5,15-bis[(4′-X-phenyl)ethynyl]-10,20-diphenylporphinato]zinc(II) derivatives, and lies ∼1400 cm^{-1} to the blue of the intense, low energy transition, consistent with its assignment as a vibronic band.[7] It should be emphasized that the Q-band region exhibits considerable spectral heterogeneity for all the [5,15-bis[(4′-X-phenyl)ethynyl]-10,20-diphenylporphinato]zinc(II) derivatives.[20] Simplex spectral fitting shows that the *x*-polarized excited states possess augmented oscillator strength and lie hundreds of wavenumbers to the red of their respective Q_y transitions.[20] These spectral assignments are consistent with the fact that conjugation is expanded about the long axis of the molecule and our electronic structure calculations (*vide infra*), which indicate that the lowest lying singlet excited states for these complexes is $Q_x(0,0)$ in nature.[20,21]

The absolute energies of the B- and Q-type transitions in the [5,15-bis[(aryl)ethynyl]-10,20-diphenylporphinato]zinc(II) complexes are also noteworthy. As a family, these porphyrins possess extensively red-shifted spectral features; the optical spectrum of [5,15-bis[(4′-dimethylaminophenyl)ethynyl]-10,20-diphenylporphinato]zinc(II) in fact displays the largest B- and Q-band bathochromic shifts of any simple *meso*-substituted (porphinato)zinc(II) complex yet reported. In general, the porphyrin B bands in the [5,15-bis[(4′-X-phenyl)ethynyl]-10,20-diphenylporphinato]zinc(II) series are red-shifted over a 2700 to 3700 cm^{-1} range relative to the B band of the unsubstituted ring system, (porphinato)zinc ($\lambda_{max,THF}$ = 398.0 nm). It is important to note that the magnitude of these shifts greatly exceeds that which can be achieved by modulation of the porphyrin axial ligand environment and illustrates the efficiency by which *meso* arylethynyl groups conjugate with the porphyrin π system.[22]

Electronic Structure of the (Porphinato)zinc(II) Complexes. In order to provide further insight into the origin of the extensive electronic perturbations derived from *meso*-arylethynyl group substitution at the porphyrin macrocycle, the orbital energies for the [5,15-bis[(4′-X-phenyl)ethynyl]-10,20-diphenylporphinato]zinc(II) complexes were determined using semiemprical methods at a configuration interaction (CI) level of 20 (see Experimental Section);[10] an analogous calculation was performed for the unsubstituted (porphinato)zinc(II) met-

(19) (a) Gouterman, M. *J. Chem. Phys.* **1959**, *30*, 1139−1161. (b) Perrin, M. H.; Gouterman, M.; Perrin, C. L. *J. Chem. Phys.* **1969**, *50*, 4137−4150.

(20) The lowest energy Q band for all the [5,15-bis[(4′-X-phenyl)-ethynyl]-10,20-diphenylporphinato]zinc(II) complexes can be mathematically fit using simplex methods as the sum of Gaussians. The amplitudes of each of these Gaussians depend on the nature of the 4′-X substituent and likely reflect the relative ambient temperature population of the maximally conjugated conformer that features coplanar ring systems with respect to those in which the arylethynyl phenyl rings and the porphyrin macrocycle assume torsional angles far removed from 0°.[21]

(21) (a) The *x*-polarized nature of the intense, low energy Q band for these complexes has been confirmed via ultrafast, singlet-excited-state anisotropy measurements. LeCours, S. M.; Jahn, L.; Therien, M. J. Manuscript in preparation. (b) Assignments of the π-π* electronic transitions at low temperature have been accomplished using MCD spectroscopy. Kirk, M. L.; Wall, M. H.; Helton, M.; Jones, R.; LeCours, S. M.; Therien, M. J. Manuscript in preparation.

(22) (a) Nappa, M.; Valentine, J. S. *J. Am. Chem. Soc.* **1978**, *100*, 5075−5080. (b) Chien, J. C. W. *J. Am. Chem. Soc.* **1978**, *100*, 1310−1312. (c) Kolling, O. W. *Inorg. Chem.* **1979**, *18*, 1175−1176. (d) Walker, F. A.; Balke, V. L.; McDermott, G. A. *Inorg. Chem.* **1982**, *21*, 3342−3348.

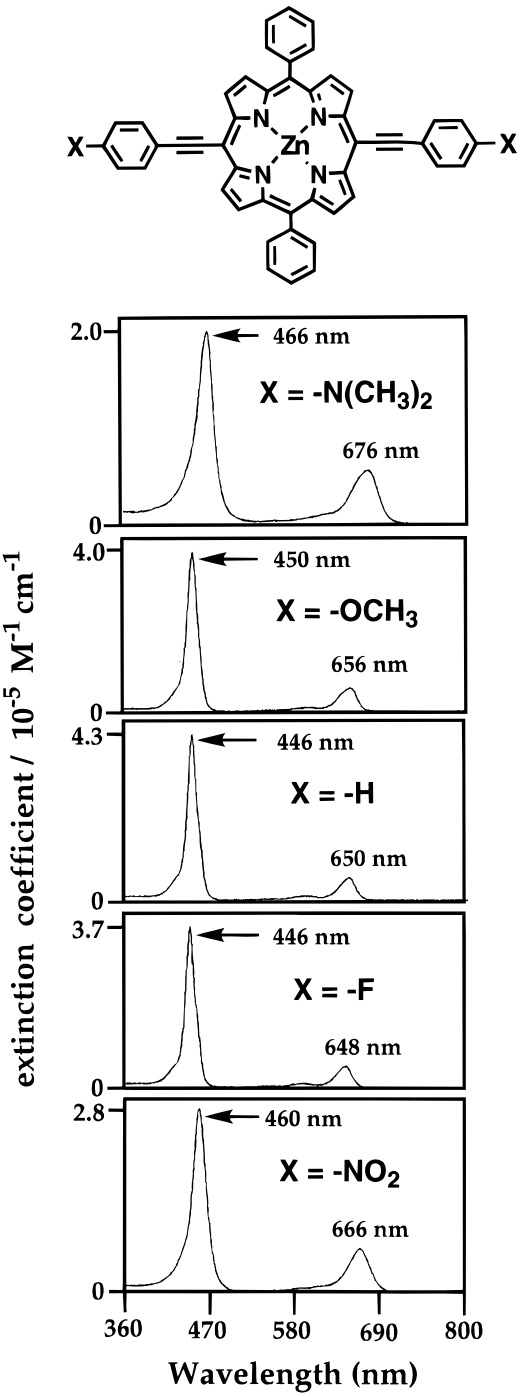

Figure 4. Electronic spectral dependence of [5,15-bis[(4′-X-phenyl)-ethynyl]-10,20-diphenylporphinato]zinc(II) complexes in THF as a function of the (aryl)ethynyl moiety's 4′-X substituent.

allomacrocycle, in order to obtain an appropriate benchmark for comparison. The results of this study are summarized in Figure 5 and Table 6; Figure 5 displays the relative energies and symmetries of the frontier orbitals (FOs) of these complexes and Table 6 lists the calculated FO energies of these species. The electron density distributions of the FOs of the [5,15-bis-[(4′-X-phenyl)ethynyl]-10,20-diphenylporphinato]zinc(II) complexes in which inductive effects dominate the electronic interaction of the 4′-substituents with the aromatic (porphinato)-zinc(II) core are similar (X = NMe_2, OMe, H, and F); the FOs of [5,15-bis[(4′-dimethylaminophenyl)ethynyl]-10,20-diphenylporphinato]zinc(II) are depicted in Figure 6 as a representative example of the members of this class of 5,15-bis[(4′-X-phenyl)ethynyl]-10,20-diphenylporphyrins. In contrast, the FOs

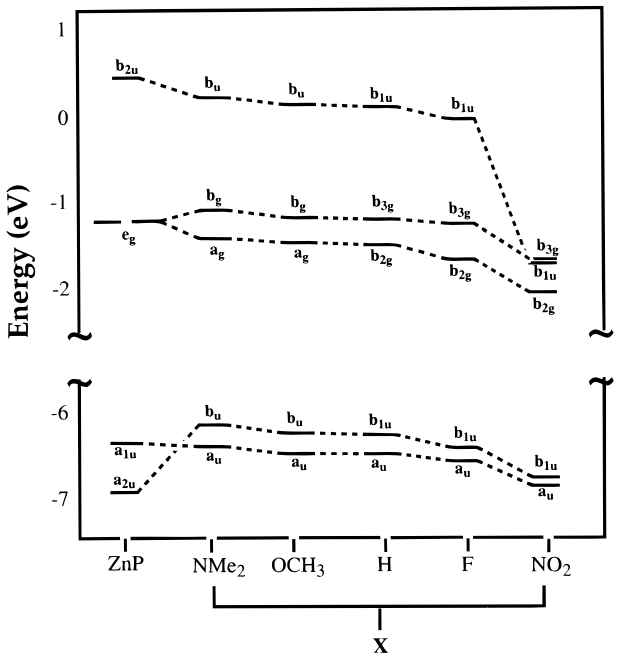

Figure 5. Evolution of the ZINDO-calculated frontier orbital symmetries and energies of [5,15-bis[(4′-X-phenyl)ethynyl]-10,20-diphenylporphinato]zinc(II) complexes relative to (porphinato)zinc(II) as a function of the electronic properties of the (aryl)ethynyl moiety's 4′-X substituent. See experimental section for computational details.

of [5,15-bis[(4′-nitrophenyl)ethynyl]-10,20-diphenylporphinato]-zinc(II) differ significantly from the other [5,15-bis[(4′-X-phenyl)ethynyl]-10,20-diphenylporphinato]zinc(II) complexes in this series in that its nitro substituents electronically communicate with both the ethynyl moieties and the porphyrin core via conjugative interactions; these FOs are shown in Figure 7. The classic Gouterman-type FOs of (porphinato)zinc(II) are displayed in Figure 8,[7] underscoring the substantive electronic differences that are manifest in the FOs of the *meso*-arylethynyl-substituted porphyrins with respect to porphyrins bearing more conventional substituents.

As seen in Figure 5, for all the [5,15-bis[(4′-X-phenyl)-ethynyl]-10,20-diphenylporphinato]zinc(II) species, the interaction of the cylindrically π-symmetric ethyne moiety with the *meso*-carbon localized electron density at the 5- and 15-porphyrin positions raises the energy of the a_{2u}-derived b_u and b_{1u} orbitals above the a_{1u}-derived orbitals having a_u symmetry. Note that the calculated energy gap (Table 6) between the HOMO-1 (the a_u orbital) and HOMO (either the b_u or b_{1u} orbital) decreases from 0.269 → 0.222 → 0.186 → 0.181 → 0.101 eV as the arylethynyl moiety's 4′-substituent is varied from NMe_2 → OMe → H → F → NO_2; thus, it is seen that as the arylethynyl phenyl rings become progressively less electron rich, the destabilizing influence of the 5- and 15-ethynyl moieties on the b_u and b_{1u} orbitals is attenuated, resulting in smaller a_u-b_u/b_{1u} electronic splitting.

Another manifestation of the cylindrically π-symmetric ethyne moiety fused directly to the 5- and 15-porphyrin *meso*-carbon positions is the considerable splitting of the formerly degenerate e_g-symmetry LUMO of (porphinato)zinc(II) (Figure 8). The calculated energy gap (Table 3) between the e_g-derived orbitals of the [5,15-bis[(4′-X-phenyl)ethynyl]-10,20-diphenylporphinato]zinc(II) complexes increases from 0.283 → 0.301 → 0.311 → 0.330 → 0.522 eV as the arylethynyl moiety's 4′-substituent is varied from NMe_2 → OMe → H → F → NO_2; the magnitude of these separations between the low-lying empty orbitals is congruent with these complexes possessing disparate Q_x and Q_y transition energies.[7] While these calculated splittings

Table 6. Calculated Frontier Orbital Energies (eV)[a] of [5,15-Bis[(4′-X-phenyl)ethynyl]-10,20-diphenylporphinato]zinc(II) Complexes Relative to (porphinato)zinc(II)

orbital	reference (porphin-ato)zinc(II)	[5,15-Bis[(4′-X-phenyl)ethynyl]-10,20-diphenylporphinato]zinc(II) complexes				
		X = NMe_2	X = OMe	X = H	X = F	X = NO_2
LUMO+2	0.491	0.197	0.106	0.080	−0.065	−1.547
LUMO+1	−1.215	−1.109	−1.176	−1.190	−1.285	−1.551
LUMO	−1.215	−1.392	−1.477	−1.501	−1.615	−2.069
HOMO	−6.344	−6.141	−6.257	−6.307	−6.411	−6.764
HOMO-1	−6.894	−6.410	−6.479	−6.493	−6.592	−6.865

[a] See Figure 5 for relevant symmetry labels.

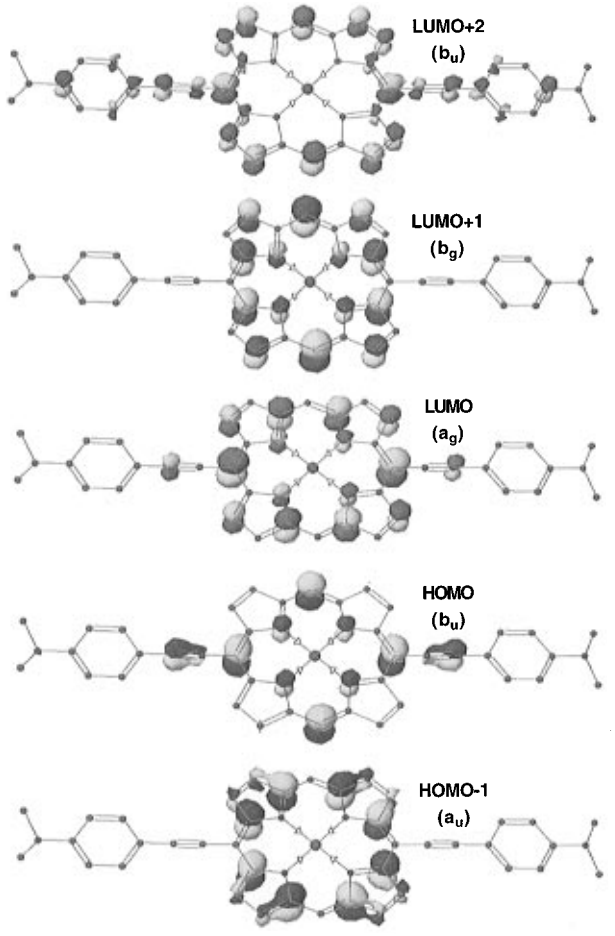

Figure 6. Frontier molecular orbitals of [5,15-bis[(4′-dimethylaminophenyl)ethynyl]-10,20-diphenylporphinato]zinc(II). The electron density centered on the 10- and 20-phenyl rings has been omitted for clarity.

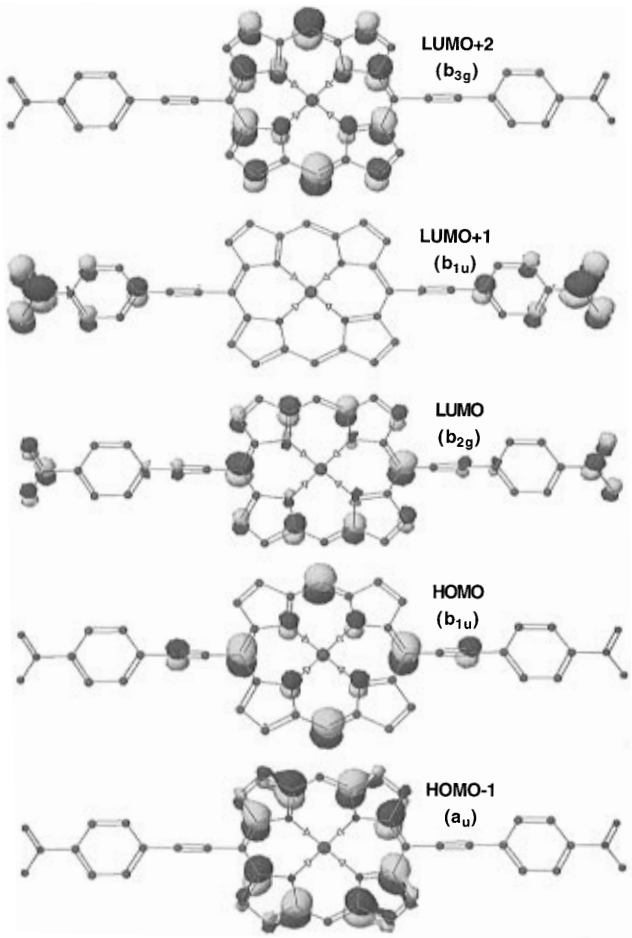

Figure 7. Frontier molecular orbitals of [5,15-bis[(4′-nitrophenyl)ethynyl]-10,20-diphenylporphinato]zinc(II). The electron density centered on the 10- and 20-phenyl rings has been omitted for clarity.

between the a_g/b_{2g}-b_g/b_{3g} orbitals (Figures 5−7) are substantial for all the [5,15-bis[(4′-X-phenyl)ethynyl]-10,20-diphenylporphinato]zinc(II) compounds, those bearing dimethylamino, methoxy, protio, and fluoro substituents possess similar LUMO-LUMO+1 energy separations with their absolute magnitude tracking with the Hammett σ_p value of the group attached to the 4′-phenyl position. When 4′-nitro substituents are utilized, more substantial splittings of the e_g-derived LUMO (b_{2g}) and LUMO+1 (b_{3g}) are realized; pendant arylethynyl moieties featuring more drastically electron deficient groups would thus be expected to both further stabilize the LUMO as well as lead to increased energy differences between the e_g-derived orbitals.

In contrast to the e_g set of (porphinato)zinc(II) (Figure 8), in which the electronic contribution of the four *meso* carbons is equivalent in each of the degenerate orbitals, the a_g/b_{2g} and b_g/b_{3g} orbitals of the [5,15-bis[(4′-X-phenyl)ethynyl]-10,20-diphenylporphinato]zinc(II) complexes evince asymmetric distributions of *meso*-carbon electron density. As shown pictorially in Figures 6 and 7, the LUMOs (a_g/b_{2g} orbitals) for these complexes show an atomic contribution from only the *meso*-carbon atoms lying along the molecular dimension of highest conjugation, while the LUMO+1s (b_g/b_{3g} orbitals) display appreciable contributions stemming from the *meso*-carbon atoms lying orthogonal to the vector defined by the two arylethynyl moieties; thus electronic excitations from filled levels into the a_g/b_{2g} and b_g/b_{3g} FOs will generate excited states that are polarized along the *x*- and *y*-molecular axes, respectively.

The LUMO+2 (b_u/b_{1u}) of the [5,15-bis[(4′-X-phenyl)ethynyl]-10,20-diphenylporphinato]zinc(II) complexes in which the 4′-substituents are either NMe_2, OMe, H, or F is calculated to lie on average 1.28 eV higher in energy than the LUMO+1. The atomic character of this FO is unusual however and merits some comment. As can be seen in Figure 6, this orbital displays significant electronic contributions from the porphyrin *meso* carbons, the ethynyl groups, and the arylethynyl phenyl rings, as well as the porphyrin β- and $C\alpha$-carbon atoms. Focusing our attention along the highly conjugated dimension of the molecule, one sees that electronic population of the LUMO+2

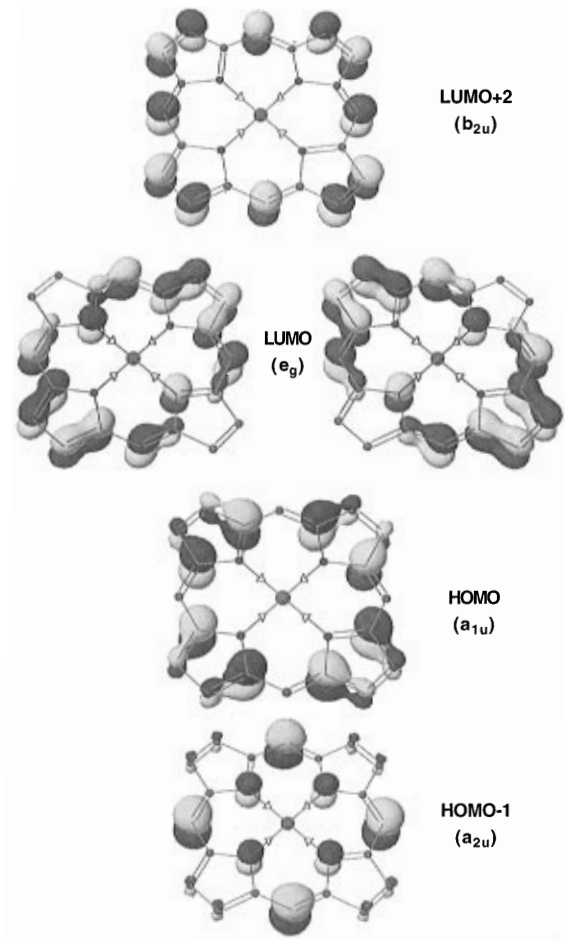

Figure 8. Frontier molecular orbitals of (porphinato)zinc(II).

will result in increased bonding interactions between the ethynyl groups and the porphyrin 5- and 15-*meso* carbon positions as well as between the arylethynyl phenyl ring C-1′ positions and the ethyne moieties; reduced bond order would be manifest in the ethyne bridge as well as in the arylethynyl phenyl rings. Optical excitation into the LUMO+2 would therefore impart significant *cumulenic character* to such a higher lying electronically excited state.

For [5,15-bis[(4′-nitrophenyl)ethynyl]-10,20-diphenylporphinato]zinc(II), the highly conjugating and electron withdrawing nitro group effects considerable stabilization of all the FOs (Figure 5; Table 6). Most conspicuous is the precipitous drop in energy of the empty b_{1u} orbital, which falls below the b_{3g} level to become the LUMO+1 (Figure 5). As a consequence of this extreme stabilization of the antibonding levels, the LUMO, LUMO+1, and LUMO+2 orbitals of [5,15-bis[(4′-nitrophenyl)ethynyl]-10,20-diphenylporphinato]zinc(II) (Figure 7) display a number of differences from those of the [5,15-bis-[(4′-X-phenyl)ethynyl]-10,20-diphenylporphinato]zinc(II) compounds that bear 4′-NMe_2, OMe, H, or F substituents (Figure 6). Firstly, significant nitro-localized electron density is present in the b_{2g}-symmetric LUMO. Secondly, in contrast to the FOs displayed for [5,15-bis[(4′-dimethylaminophenyl)ethynyl]-10,20-diphenylporphinato]zinc(II) (Figure 6), it is the LUMO, not the LUMO+2 of [5,15-bis[(4′-nitrophenyl)ethynyl]-10,20-diphenylporphinato]zinc(II) that evinces extensive cumulenic character. Thirdly, the *ungerade* empty FO (Figure 7) is essentially localized on the arylethynyl nitrophenyl moieties and bears little porphyrinic electronic constitution. Finally, as seen in Figure 7, the LUMO and LUMO+1 now possess augmented *x*-polarized electron density; the formation of *y*-polarized excited states now requires electronic population of the LUMO+2. While promotion of electrons into the empty b_u/b_{1u} levels from the a_u and b_u/b_{1u} orbitals of the [5,15-bis[(4′-X-phenyl)ethynyl]-10,20-diphenylporphinato]zinc(II) compounds will give rise to lower oscillator strength transitions relative to those involving the empty a_g/b_{2g} and b_g/b_{3g} sets due to their symmetry forbidden nature, excitations involving the b_u/b_{1u}-derived levels in electronically asymmetric arylethynylporphyrins would be predicted to significantly impact the nature of the excited states of such complexes, particularly if at least one porphyrin *meso* substituent, such as a (4′-nitrophenyl)ethynyl moiety, served to stabilize such an orbital.[23,24]

Table 7 compares the experimental electronic spectral data for the [5,15-bis[(4′-X-phenyl)ethynyl]-10,20-diphenylporphinato]zinc(II) species with the theoretically determined transition energies derived from ZINDO CI calculations. Note that the calculated electronic spectral transitions mirror the salient features displayed in Figure 4, namely that the energies of the B- and Q bands progressively blue shift as the 4′-substituents of the [5,15-bis[(4′-X-phenyl)ethynyl]-10,20-diphenylporphinato]zinc(II) complexes become less electron donating throughout the series X = NMe_2, OMe, H, F; moreover, these calculations are consistent with experiment in that the energy separating the most intense visible transitions increases in the order NMe_2 < OMe < H < F for the 4′-X substituents. When the 4′-substituent is changed to the even more electron withdrawing X = NO_2 group, theory and experiment evince abrupt spectral red shifts of the B- and Q-band transitions coupled with a decrease in the B-Q spectral splitting with respect to the 4′-X = F derivative (Table 7). While this behavior for the 4′-X = NO_2 complex is predictable *a priori* since the porphyrin-centered π-π^* transitions should shift to lower energy as conjugation is expanded out onto the nitro moieties, it is gratifying that these electronic structure calculations correctly predict how each of the 4′-X substituents perturbs the optical spectrum of their respective [5,15-bis[(4′-X-phenyl)ethynyl]-10,20-diphenylporphinato]zinc(II) complexes. Moreover, this dramatic reordering of the FO energies and electron distribution is concordant with the exceptional nonlinear optical properties reported for porphyrins bearing the 4′-NO_2-phenyl)ethynyl electron acceptor.[23−24]

These electronic structure studies are consistent with the high oscillator strength B- and Q bands having substantial $B_x(0,0)$ and $Q_x(0,0)$ character. The disparity in oscillator strength between the *x*- and *y*-polarized absorptions has its genesis in the removal of the degeneracy of the porphyrin LUMO which gives rise to transition dipoles corresponding to the lowest singlet excited configurations that differ substantially in magnitude, consistent with the essential features of the classic Gouterman four-orbital model.[3d,7,18] Previously performed INDO/SCI calculations which examined excited-state wave functions of a donor-acceptor version of the 5,15-bis[(aryl)-ethynyl]-10,20-diphenylporphyrin structural motif quantitatively made a similar prediction, estimating the oscillator strength of the $Q_x(0,0)$ transition to be approximately ten times that of the $Q_y(0,0)$ absorption with the $B_x(0,0)$ thrice that of the $B_y(0,0)$.[24]

Summary and Conclusion

Removing the steric barrier to rotation between the porphyrin core and its pendant aryl substituents through an intervening ethynyl moiety allows considerable tuning of the porphyrin frontier orbital energies. Our work demonstrates that porphyrin *meso*-arylethynyl groups can be utilized to significantly regulate

(23) LeCours, S. M.; Guan, H.-W.; DiMagno, S. G.; Wang, C. H.; Therien, M. J. *J. Am. Chem. Soc.* **1996**, *118*, 1497−1503.
(24) Priyadarshy, S.; Therien, M. J.; Beratan, D. N. *J. Am. Chem. Soc.* **1996**, *118*, 1504−1510.

Table 7. Comparison of Experimental and Calculated Electronic Spectral Features of [5,15-Bis[(4′-X-phenyl)ethynyl]-10,20 diphenylporphinato]zinc(II) Complexes

compd	B band λ_{max},[a] (exp., eV)	Q band λ_{max}[b] (exp., eV)	spectral splitting[c] (exp., eV)	B band λ_{max},[a] (calc., eV)	Q band λ_{max}[b] (calc., eV)	spectral splitting (calc., eV)
(porphinato)Zn	3.10	2.22	0.88	3.80	2.15	1.65
X = NMe_2	2.66	1.83	0.83	3.33	2.01	1.32
X = OMe	2.75	1.89	0.86	3.41	2.01	1.40
X = H	2.78	1.91	0.87	3.43	2.02	1.41
X = F	2.78	1.91	0.87	3.44	2.02	1.42
X = NO_2	2.70	1.86	0.84	3.13	2.00	1.13

[a] Refers to the B(0,0) transition for (porphinato)zinc(II) and the intense, B transition for the [5,15-bis[(4′-X-phenyl)ethynyl]-10,20-diphenylporphinato]zinc(II) complexes which has augmented $B_x(0,0)$ in character. Experimental values determined in THF solvent. [b] Refers to the Q(0,0) transition for (porphinato)zinc(II) and the Q transition for the [5,15-bis[(4′-X-phenyl)ethynyl]-10,20-diphenylporphinato]zinc(II) complexes which has augmented $Q_x(0,0)$ in character. Experimental values determined in THF solvent. [c] Defined as the energy separation between the respective B and Q bands.

chromophore spectroscopic properties as well as macrocycle electrochemical properties. A unique aspect of these [5,15-bis-[(4′-X-phenyl)ethynyl]-10,20-diphenylporphinato]zinc(II) systems lies in the fact that this extensive electronic modulation was achieved at an undistorted, planar macrocycle through substitution at only two points on the porphyrin periphery. Such arylethynyl-substituted porphyrins will allow wide-ranging substituent electronic effects to be evaluated independently of porphyrin core structural perturbations. Moreover, this chemistry defines a general method for regulating the optoelectronic properties of long wavelength absorbing dyes. Studies of the photophysical, magnetic, electrochemical, ground- and excited-state vibrational properties, as well as further work focused on the details of the electronic structure of other metal derivatives of these and similar systems will be the subjects of future publications.

Acknowledgment. M.J.T. is indebted to the Searle Scholars Program (Chicago Community Trust), the Arnold and Mabel Beckman Foundation, E. I. du Pont de Nemours, and the National Science Foundation for Young Investigator Awards as well as the Alfred P. Sloan Foundation, the National Institutes of Health (GM 48130-01A1.4), the U.S. Department of Energy (DE-FGO2-94ER14494), the Office of Naval Research (96-1-0725), and the Exxon Education Fund for their generous financial support.

JA962403Y